Mass Transfer in Liquid-Lithium Systems

WILLIAM N. GILL, RICHARD P. VANEK, ROBERT V. JELINEK, and C. S. GROVE, JR.

Syracuse University, Syracuse, New York

The behavior of type-304 stainless steel in a forced-convection closed-loop lithium system was investigated over a wide range of temperatures and velocities. Fundamental information concerning the mechanism for mass transport has been obtained by examining solution and deposition effects along flat plates. The rate-determining process for solution is transport from the solid to the interface, whereas deposition rates are liquid-phase controlled.

Liquid-phase mass transfer coefficients were correlated with a maximum deviation of approximately 15% by the use of von Kàrmàn's analysis of the turbulent boundary layer along a flat plate, combined with the Chilton-Colburn empirical modification of the Schmidt group. In contrast no adequate model is available for the prediction of solution rate constants which must be determined experimentally. Mean values of the solution rate constants ranged from 0.154 to 0.750 x 10^{-5} cm./sec. at temperatures from 510° to 612°C. These values are on the order of 10^{3} smaller than corresponding liquid-phase mass transfer coefficients.

Significant theoretical developments and quantitative data relating to liquid-metal heat transfer are available. Comparable contributions for mass transport phenomena, except for mercury systems, have not been forthcoming. Several studies have provided qualitative data about the corrosive effect of liquid alkali metals and their compounds on various materials of construction. Descriptive information is available concerning thermal-gradient mass transfer in lithium systems for both natural and forced convection (*1, 2, 3*). These studies suggested general solution as the principal over-all mechanism for mass transfer to the fluid phase. Other types of corrosion have been observed (*4*) which contribute to some extent to the total transport of material.

Epstein (*5*) investigated the mass transfer problem in dynamic-sodium and mercury-loop systems by employing quantitative techniques. Two mechanisms for corrosion were considered. The rate-determining step for solution-limited corrosion is the transfer of material from the metal surface to the adjacent liquid boundary layer. For the diffusion-limited mechanism the rate of transfer of material through the liquid boundary layer controls the process. The principal difference between these mechanisms is that the interfacial liquid concentration is in equilibrium with the solid phase in the diffusion-limited case, whereas it is not saturated and is approximately equal to the average bulk-stream concentration in solution-limited corrosion. The mercury-iron and sodium-iron systems are described respectively as diffusion limited and solution limited.

Dunn *et al.* (*6*) studied mass transfer rates for metals quite soluble in mercury at room temperature. The data were correlated by use of the various dimensionless correlations applicable to the systems studied. Linton and Sherwood (*7*) investigated the solution of tubes and plates for both laminar and turbulent flow. This investigation represented a considerable extension of mass transfer data to higher values of $(\mu/\rho D_L)$, and the data were correlated by use of conventional dimensionless equations.

A recent study by Bennett and Lewis (*8*) discusses the applicability of boundary-layer analysis and the more recently developed surface-renewal theory (*9, 10*). It has been shown (*11*) that the laminar-sublayer and surface-renewal models yield similar equations, and thus mass transport may be expressed in traditional form independent of the frame of reference used. To test these theories, two designs of apparatus were used in the experiments by Bennett and Lewis, and two equations were employed to correlate the data, depending on the method used. Although an exponent of 0.5 for the Schmidt group (as predicted by the surface-renewal theory) was applicable to one system, this was not considered sufficient evidence to confirm or reject the surface-renewal theory.

EXPERIMENTAL PROCEDURE

The apparatus employed is shown schematically in Figure 1. Lithium was charged to the hold tank through a sintered stainless steel filter with 5-μ pore size. The entire system was pretreated with low-temperature lithium to reduce surface films. Type-304 stainless steel plates (1 by ⅝ by 1/16 in.) which had previously been electropolished to eliminate surface films were arranged to form a continuous flat plate parallel to the direction of flow. This was accomplished with ⅝-in. tubes 27-in. long which were machined to hold ten to twenty-five plates rigidly to form one continuous plate. The ⅝-in. tube together with the inserted plates was placed inside a ¾-in. tube and the assembly locked together to hold the two tubes concentrically.

Lithium flowed parallel to both sides of the plate causing material to be transferred identically on both sides. This arrangement enabled the measurement of mass flux to and from plates 1 to 25 in. long under invariant conditions for a given run. The temperature and flow conditions were altered as desired for different runs. Plate assemblies were varied in length from 10 to 25 in. Two test sections were incorporated in the system; one was placed in the hottest and the other in the coldest part of the system. During all runs the low-temperature test section was maintained at a constant temperature, whereas both isothermal and nonisothermal conditions were established in the hot section. As expected, material was transferred from the plates to the liquid stream in the hot zone and from the liquid stream to the plates in the low-temperature section.

The lithium used was high-purity vacuum-distilled material reported to have the following analysis:

Lithium analysis

Na	K	Ca	N	Fe	Li
0.005%	0.01%	0.02%	0.06%	0.001%	99+%

During each run lithium was filtered continuously to reduce contamination and to justify the assumption of a steady state concentration distribution; the outlet stream from the filter was assumed to be saturated at the filter temperature. The filter also served to remove particulate matter resulting from crystal growth in the liquid stream. In addition the lithium was filtered continuously at approximately 0.5 to 1°C. above its melting point at the termination of each run to maintain contamination at a low level. The absolute magnitude and consistency of results indicate that this is an effective procedure and that catalytic effects due to oxides and nitrides were minimized. It is concluded that continuous filtration is probably the single most fruitful method to obtain consistent and reliable experimental results.

The entire system was made of type-304 stainless steel with the exception of the fittings which were of type-316 stainless steel. A single material was used to eliminate dissimilar metal transfer which would undoubtedly bias the results. A preliminary study on static isothermal assemblies indicated that austenitic stainless steels were superior to other stainless steels. Also a statistical analysis of the results showed no significant differences between type-304 and the other series-300 steels up to 500°C. Refractory metals, which are more inert, present considerable experimental difficulty because of oxidation problems unless the entire system is operated in an inert atmosphere. Therefore type-304 stainless steel was chosen for this investigation, despite its complexity, because of its practical importance in handling lithium. Small fluxes could be anticipated with this material, which satisfied most assumptions made in theoretical investigations. The principal limitation in using a complex alloy is that several components, rather than one, are

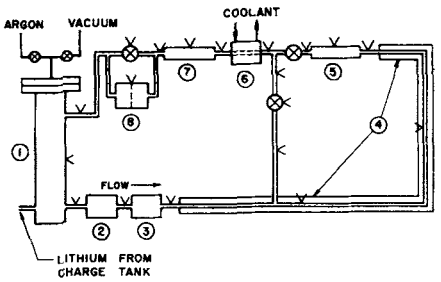

Fig. 1. Closed-loop mass transfer system: 1—surge tank, 2—electromagnetic pump, 3—electromagnetic flowmeter, 4—heating section, 5—hot sample section, 6—cooler, 7—cold sample section, 8—filter, v —thermocouple, ⊗—valve.

transferred simultaneously. Consequently mean diffusivities must be used in the calculations, but this is not a severe limitation because the diffusivities of iron, nickel, and chromium in liquid lithium are about equal, as indicated by the Stokes-Einstein equation.

Thermocouples positioned at various points in the system measured the temperature distribution. The temperature in each sample section and throughout the system was measured periodically by use of a K-2 potentiometer and also monitored continuously on a multipoint recorder.

An electromagnetic pump circulated the lithium, and a calibrated electromagnetic flowmeter measured the fluid velocity. This type of pump is particularly convenient for experimental work with liquid metals, since it provides excellent velocity control and reliable operation.

After a specified time, from 67 to 100 hr., the plates were removed, and the mass flux was measured by weight difference. Photomicrographic, X-ray, and chemical analyses were employed to determine structural changes occurring in the solid phase and to identify the components transferred. Crystals were also cold trapped upstream of the filter and analyzed for this purpose.

MASS FLUX AND THE TRANSPORT MECHANISM

Theory

In most liquid lithium mass transfer investigations the material transported is the containing system. Therefore the solubility levels of interest are on the order of parts per million. Changes in the bulk-stream concentration around the system can be less than 1 part/million as in this investigation. This precludes direct measurement of concentration differences by chemical means and requires the use of a different method. It is desirable to formulate equations describing the process in terms of mass flux at the phase boundary which can be measured directly. With known fluxes concentration distributions can be deduced from the continuity equations.

Bird (*12*) discusses various frames of reference for defining fluxes and clearly presents the relationships between them. The nature of turbulence and its role in thermal and material transport are described by Opfell and Sage (*13*). On the basis of the general equations described in these monographs it is easily shown that

$$V_z \frac{\partial C_L}{\partial z} = \bar{\Sigma}_{d,K} \frac{1}{r} \frac{\partial}{\partial r}\left(r \frac{\partial C_L}{\partial r} \right) \quad (1)$$

for steady flow of an incompressible fluid in a constant cross-sectional area, circular conduit. Solutions to the heat transfer analogue of Equation (1) have been obtained for plug, laminar, and turbulent flow in tubes by Lévèque, Graetz, and Latzko (*14*) assuming constant physical properties. These solutions have been compared with experimental data with considerable success (*14, 15*).

Practical problems are usually complicated by large thermal gradients and the nature of the solid phase, when this offers appreciable resistance to transfer. This has made it necessary to state the continuity equation in the simplest possible form so that it can be integrated over the system considered. It is desirable to examine this approach for circular tubes, since the procedure was used in this study. The macroscopic steady state continuity equation for each component in the liquid stream is

$$\frac{dC_L}{dz} = \left[\frac{A_p}{V_{av} A_c} \right] N_r \quad (2)$$

In addition local mass transfer coefficients, for steady state conditions, are defined for each component by

$$N_r = k_s(C_s - C_s^*) \quad (3a)$$
$$= k_c(\gamma^\circ C_L^\circ - \gamma C_L^*) \quad (3b)$$
$$= k_L(C_L^* - C_L) \quad (3c)$$

Equations (3*a*), (3*b*), and (3*c*) describe solid-phase diffusion, interfacial chemical rates, and liquid-phase diffusion, respectively. It should be noted that γ° and C_L° in Equation (3*b*) refer to quantities in thermodynamic equilibrium with the solid phase immediately adjacent to the liquid; this may not be identical with the bulk solid.

Solution Phenomena Epstein (5) suggested two distinct mechanisms for

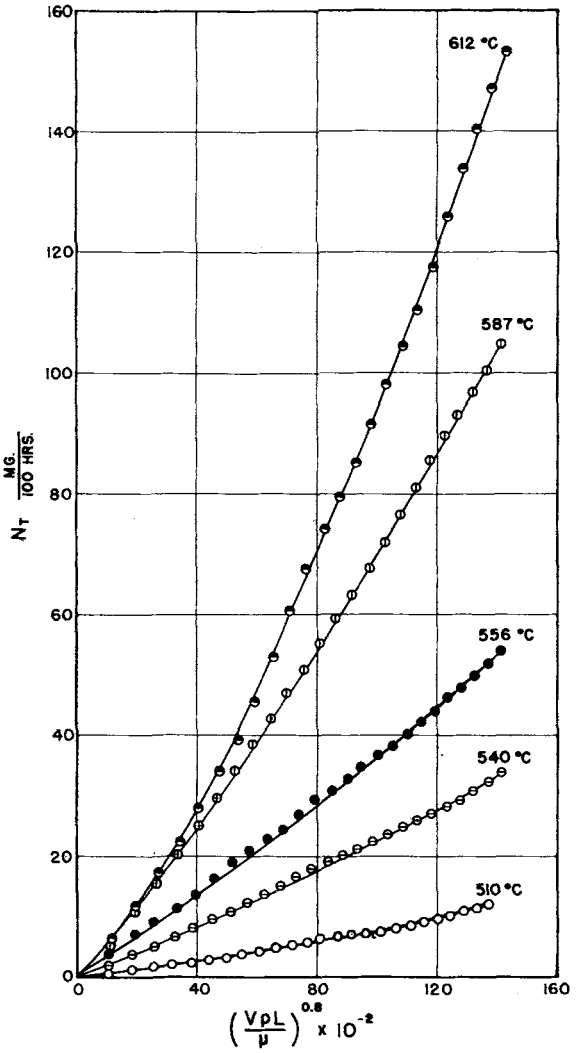

Fig. 2. Solution of flat plates in lithium (variation of mass flux with Reynolds number).

- ⊖ 612°C.
- ⊙ 587°C.
- ● 556°C.
- ⊖ 540°C.
- ○ 510°C.

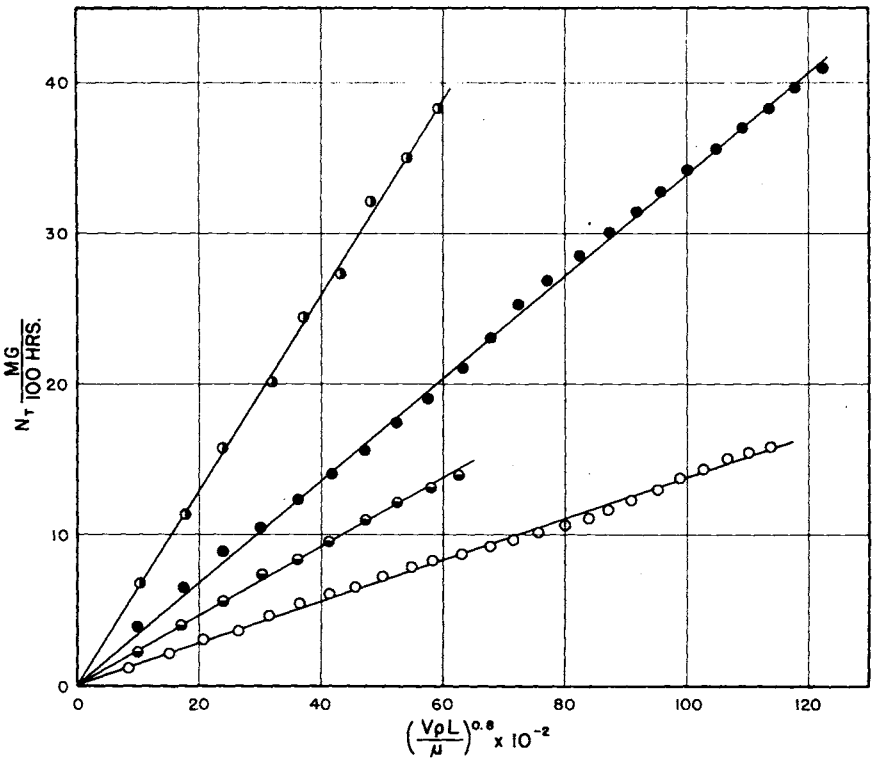

Fig. 3. Deposition on flat plates from lithium (variation of mass flux with Reynolds number).
- o 490°C.
- • 450°C.
- o 445°C.
- o 328°C.

solution phenomena in liquid-metal systems as previously described. The diffusion-limited mechanism controls for single-component solids, where k_c is large and C_L^* is approximately equal to C_L°. It is readily seen that these conditions give directly

$$N_r = k_L (C_L^\circ - C_L) = k_L (C_L^* - C_L) \qquad (3c)$$

Hydrodynamic effects are most pronounced for systems that can be so described. This behavior has been observed in mercury systems with iron, tin, lead, and cadmium solutes (6, 8). When the interfacial liquid boundary-layer cannot be considered saturated, several possibilities arise and have been observed experimentally. For pure solids the chemical-rate factor may enter into the solution process as observed with zinc in several solvents (8). Also the solution rate may be affected by the existence of a solid boundary layer of reaction products resulting from a chemical reaction between the solid and an impurity of the liquid or the liquid itself. The iron-sodium system exhibits this behavior (5). Solution of multicomponent solid alloys is further complicated by solid-phase diffusion. All these effects are included in an over-all mass transfer coefficient frequently designated a "solution-rate constant," and the mass flux is written

$$N_r = \alpha(C_L^\circ - C_L) \qquad (4)$$

If the origin of the coordinate system is chosen at a point in the system where the liquid stream is saturated, that is the outlet from the filter, the flux distribution around the system can be obtained directly. Differentiating Equation (4), combining this with Equation (2), and integrating with the condition $N_r=0$ at $z=0$ (at the filter outlet this condition is satisfied since the bulk stream is saturated), one obtains

$$N_r = \alpha_m e^{-\lambda_m z} \int_0^z \left(\frac{dc_L^\circ}{dT}\frac{dT}{dz}\right) e^{\lambda_m z} dz \qquad (5)$$

where

$$\lambda_m = \frac{A_p\ \alpha_m}{V_{avg} A_o}$$

If analytical expressions are available for the temperature coefficient of solubility and the temperature distribution in the system, the integral is easily evaluated; α_m and λ_m are best determined by

$$\lambda_m = \frac{1}{z}\int_0^z \lambda(z)\, dz \qquad (6)$$

Epstein (5) simplified Equation (5) by assuming that $(dC_L^\circ)/(dT)$ was essentially constant over small temperature intervals and that the temperature distribution can be approximated by a simple cosine function. Employing these assumptions, one obtained order-of-magnitude agreement.

Deposition Phenomena For deposition processes only k_c and k_L need be examined. If k_c is large, as it is shown to be for the system investigated, the interfacial liquid is assumed to be in thermodynamic equilibrium with the solid. Consequently the mass flux can be written as

$$N_r = k_L(C_L - C_L^\circ) = k_L(C_L - C_L^*) \qquad (7)$$

Since the transfer mechanism cannot be observed directly, it must be determined by inference. Transport in turbulent flow parallel to a flat plate is ideal for this purpose. This system has been the subject of considerable theoretical investigation, particularly as it relates to heat and momentum transfer. Von Kàrmàn (16) studied the heat transfer problem. From a heat balance over the boundary layer, based on the 1/7 power velocity distribution law, he derived the following relationships for local and total fluxes respectively:

$$q_r = 0.0285\ \rho C_p V_o \theta \left(\frac{\mu}{\rho V_o x}\right)^{0.2} \qquad (8)$$

$$q_T = 0.0356\, \mu\, C_p\, \theta_o \left(\frac{\rho V_o L}{\mu}\right)^{0.8} \qquad (9)$$

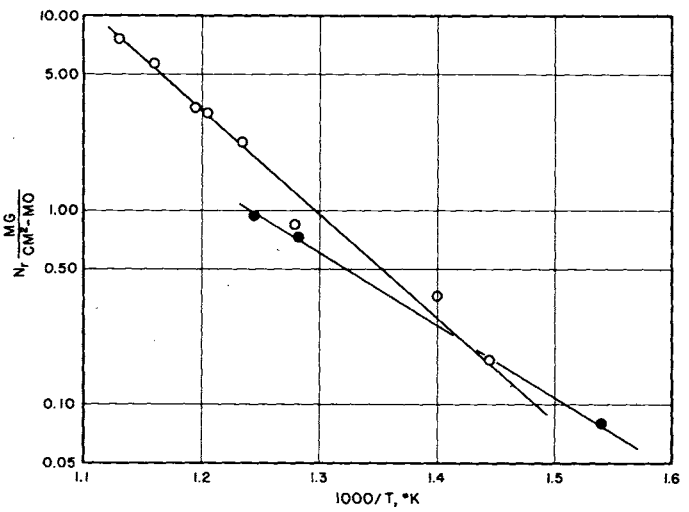

Fig. 4. Variation of mass flux with temperature.
- o present data on lithium
- • data of Epstein (5) on sodium

TABLE 1. CONDITIONS FOR SOLUTION-RATE DATA IN FIGURE 4

N_T (mg./sq. cm.-mo)	$T_{soln.}$, °C.	T_{filter}, °C.	ΔT, °C.	Time, hr.	V, cm./sec.	Type of specimen dissolving
			Lithium			
7.6	612	490*	122	100	15.5	plate
5.7	587	450*	137	100	15.5	plate
4.7	583	548*	35	100	40.0	plate
3.4	563***	543	20	100	60.0	tube
3.15	556	445*	111	67	15.5	plate
2.21	541	328*	212	100	15.5	plate
0.85	510	374	136	100	15.5	plate
0.36	440**	430	10	100	85.0	plate
0.17	421**	374	45	100	85.0	plate
			Sodium			
0.94	535	425	110	—	30	
0.71	500	460	40	—	60	
0.08	375	225	150	—	45	

* Deposition rates were measured at these conditions and are shown in Figures 3 and 5.
** Preliminary measurements were made to determine the temperature level necessary to obtain reliably reassurable rates.
*** Fifteen measurements on tubes were made under these conditions to test the assumption that the solution rate is independent of geometry.

Von Kàrmàn's analysis assumes a stream of infinite extent, where the main stream above the boundary layer is undisturbed. This is approximated by flat plates in tubes along a relatively short length before the tube-and-plate boundary layers interact. By analogy it would be expected, for a given ΔC_o, that the total mass flux over the length is proportional to $[(V_oL)/\nu]^{0.8}$ for an isothermal system if the fluid resistance predominates. Conversely, if the transfer process is controlled by crystal orientation or solid-phase diffusion effects, the growth of the boundary layer should affect mass transfer to a lesser extent and the rate is essentially independent of the fluid velocity and directly proportional to the length of the plate.

Experimental Results

Mass-Flux Data Figures 2, 3, and 4 are representative mass-flux data obtained in this study. The behavior of each individual curve in Figures 2 and 3 is independent of the driving force, since this is constant for a given curve. Figure 2 shows fluxes from the plates to the lithium stream. All runs indicate some degree of positive curvature, and this curvature increases with increased flux as expected for solution-limited transfer.

In contrast Figure 3 for fluxes to the plates corroborates von Kàrmàn's predicted effect of the Reynolds number. It is seen that the total flux in this case is linear in $[(V_oL)/\nu]^{0.8}$ within experimental error. This suggests a solid-phase controlled-solution process and a fluid mechanically controlled precipitation process. Subsequent examination of mass transfer coefficients and solution-rate constants corroborates this. In large measure this explains the plugging phenomena observed in nonisothermal closed-loop systems. Since the precipitation process is rapid relative to the solution process, the deposition of material in the system is limited only by the concentration or activity potential available.

Each point in Figure 4 is based on twenty-five observations of solution rates under a given set of conditions. It is seen that the mass flux is substantially linear in $1/T$, despite the variation in temperature differences and velocities shown in Table 1. This experimental result strongly suggests that the observed solution rate, under the range of conditions investigated, is an exponential function of the solution temperature. This is quite reasonable considering that a large number of diffusion processes, reaction-velocity constants, and solubility concentrations can be expressed by an Arrhenius type of equation over limited temperature ranges. An identical result was obtained for the mercury-iron system (5), and the reasons for this were discussed rather extensively.

Figure 4, together with the temperature distribution, can be employed to determine the concentration distribution around the system with the continuity equation used in the form

$$C_L = C^\circ_{filter} + \frac{A_p \int_o^L N_T dz}{V_{avg} A_c} \quad (10)$$

The stream leaving the filter is assumed to be saturated.

Mass Transfer Coefficients. A search of the diffusion literature (17) on liquid metals led to the conclusion that measured diffusivities were one to two times those calculated with the Stokes-Einstein equation:

$$\frac{D_L \mu}{T} = \frac{K}{6R_A \pi} \quad (11)$$

This then provides a reasonable approximation for use in dimensionless correlations to predict mass transfer coefficients.

The atomic radii of iron, nickel, and chromium are 1.26, 1.24, and 1.25 Å. respectively, and therefore diffusivities of these elements in dilute solutions should, on the basis of the Stokes-Einstein equation, be essentially the same. A value of 1.25 Å. was used to calculate the mean diffusivity.

Von Kàrmàn's analysis modified for mass transfer as a Chilton-Colburn j-factor correlation leads to

$$j_d = 0.0356\ (N_{Re_L})^{-0.2} \quad (12)$$

or, with a slightly modified friction

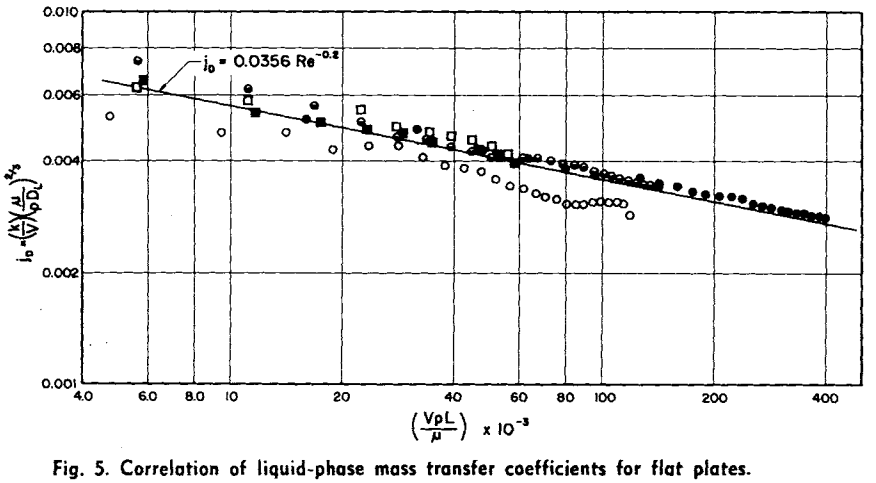

Fig. 5. Correlation of liquid-phase mass transfer coefficients for flat plates.

	Temp., °C.	Velocity, cm./sec.	Plate length, cm.	ΔC x 10⁴ mg./cc.
□	445	15.5	2.54-25.4	1.30
■	490	15.5	2.54-25.4	3.63
○	328	15.5	2.54-63.5	1.17
⊙	450	15.5	2.54-63.5	2.00
●	548	40.0	2.54-63.5	1.38

factor for smooth flat plates as suggested by Schlichting (*18*), to

$$j_d = 0.0370\ (N_{Re_L})^{-0.2} \qquad (13)$$

The coefficients in these relations are mean values over the plate length.

Since the filter and cold-section plates were maintained at the same temperature, the equilibrium solubility was the same in both. In addition if the deposition process is fluid mechanically controlled, as suggested by the previous discussion of von Kàrmàn's analysis, the interfacial concentration at the plate is an equilibrium value identical with the outlet concentration of the filter. Consequently the driving force for deposition is equal to the increase in concentration experienced by the lithium in travelling from the filter outlet to the plate entrance. These values are given in Figure 5. Therefore mass transfer coefficients were calculated by the use of

$$k_L = \frac{N_r}{A\Delta C_o} \qquad (14)$$

where ΔC_o is determined with Equation (10) and measured solution rates used.

The data falling below the solid line in Figure 5 were all obtained at 328°C., whereas the data on or above the line represent temperature between 445° and 548°C. No consistent bias is observable in the higher-temperature data, and the experimental error is apparently small. The larger deviations from predicted values for the 328°C. data are probably due to error in ΔC_o. The temperature gradient throughout the heat exchanger was particularly high for the 328°C. data (8.5°C./in.) and may have caused a significant decrease in the concentration of the stream approaching the plates via deposition in the exchanger. This may account for the low experimental values of k_L.

TABLE 2. SOLUTION-RATE CONSTANTS

$\alpha_m \times 10^5$, (cm./sec.)*	$\alpha \times 10^5$, (range)*	ΔC, mg./cc.	t, °C.	Δt system, °C.	$N_{Re} \times 10^3$
0.154	0.204-0.142	0.129	510	136°C	6-150
0.299	0.398-0.259	0.206	541	212°C	6-154
0.504	0.775-0.428	0.204	556	111°C	6-155
0.670	0.764-0.616	0.289	587	137°C	6-160
0.750	0.792-0.694	0.331	612	122°C	6-163

* The mean values and ranges for solution-rate constants were based on twenty-five measurements in all cases.

These data contrast with those obtained by Linton and Sherwood (*7*). For plates their results in all cases were 1.5 to twofold above the solid line in Figure (5). These authors logically suggest that this is attributable to the induced roughness of the plates caused by solution effects. This is a reasonable conclusion as discussed extensively by Schlichting (*18*).

Solution-Rate Constants. Unlike the mass transfer coefficients discussed previously for fluxes to the solid phase, the mechanism for solution is not readily discernible because of its inherent complexity and the lack of sufficient solubility data. Solubility data were obtained for nickel from the the work of Bagley and Montgomery (*19*) and for iron from Sand *et al.* (*20*). No chromium solubility data were available. Therefore the solution-rate constants shown in Table 1 were calculated on the basis of these data. It is readily seen that the absolute magnitude of the solution rate constants is smaller, by a factor of 10^3, than expected for diffusion-limited processes. A simple calculation with the approximate relationship

$$\frac{1}{\alpha} = \frac{1}{k_L} + \frac{1}{\gamma^\circ k_c} + \frac{1}{Kk_s} \qquad (15)$$

shows that

$$\frac{1}{\alpha} \approx \frac{1}{\gamma^\circ k_c} + \frac{1}{Kk_s} \qquad (16)$$

within less than 1%. Therefore the solution-rate constant is dependent on the solid phase and interfacial resistances only.

The proper driving force to use for solution-rate constant calculations is the difference between the equilibrium concentration and the bulk-stream concentration. This is exactly equivalent to the difference in solubility between the solution temperature and the filter temperature plus the bulk-stream concentration increase caused by solution between these points. These values are given in Table 2. According to Figure 4 log N_r is essentially linear in $1/T$. Therefore the solution-rate constants should be linear in this variable. This condition is only approximately satisfied. Deviations from linearity are probably attributable to the lack of complete solubility data.

It is clear from the behavior of the individual solution-rate constants* that the solution process is controlled primarily by the solid phase, in contrast to the precipitation process. Although there is a slight tendency for these constants to decrease with increasing Reynold's number, this is not nearly so pronounced as that observed in fluid mechanically controlled systems.

Solid-Phase Analysis. The photomicrographs in Figure 6 provide a means of estimating quite accurately the depth of deposition product layers due to mass transfer in the low-temperature section of the system. The band above the stainless steel substrate represents the deposition layer. It can be seen that this layer is well delineated, and no diffusion into the substrate is evident. Fluxes observed by weight differences for Figure 6*a* and *b* were in the ratio of 1/2.83, which corresponds to the respective band widths shown. The exact structure of the de-

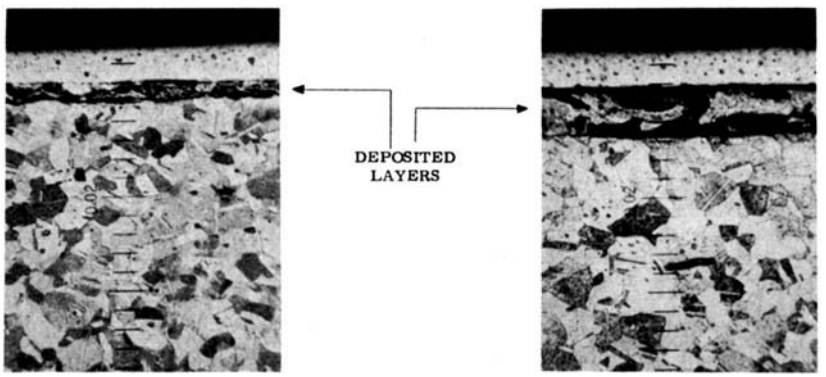

a

MAX. SYSTEM TEMPERATURE (556°C)
DEPOSITION TEMPERATURE (445°C)
3 divisions = 0.002 in.
x 300

b

MAX. SYSTEM TEMPERATURE (612°C)
DEPOSITION TEMPERATURE (490°C)
3 divisions = 0.002 in.
x 300

Fig. 6. Photomicrographs showing deposition layer.

* Tabular material has been deposited as document No. 6125 with the American Documentation Institute, Photoduplication Service, Library of Congress, Washington 25, D.C., and may be obtained for $1.25 for photoprints or for 35-mm. microfilm.

position products is difficult to determine, but spectrographic analysis of crystals trapped upstream of the filter showed that nickel was the principal component transferred and that chromium, manganese, silicon, and carbon were present in detectable amounts.

X-ray diffraction and photomicrographic analysis of the plates in the high-temperature section of the system where solution occurs showed transformation of the austenitic structure to a ferritic structure. Corresponding to mass-flux rates, the degree of conversion to ferrite increased rapidly with temperature. In an inert atmosphere the austenitic structure of type 304 stainless steel is quite stable at 600°C.; therefore transformation to ferrite can be attributed to the preferential loss of nickel, which is the major stabilizing component for austenite in type-304 stainless steel. Precipitation of chromium carbide at grain boundaries, thereby depleting the matrix of carbon, also enhances ferrite formation.

CONCLUSIONS

1. Mass transfer coefficients in alkali metal systems for fluxes to the solid phase are predicted within experimental error by von Kàrmàn's theoretical analysis of the turbulent boundary layer for flow parallel to a flat plate, combined with the Chilton-Colburn empirical modification of the Schmidt group.

2. The fundamental transfer mechanism is unaltered by the system geometry. Therefore j-factor correlations would be expected to predict mass transfer coefficients in circular tubes.

3. Mass transfer from the solid to the liquid stream is controlled by solid-phase diffusion and cannot be predicted from correlations based on liquid-phase diffusion.

4. No interfacial chemical resistance was evident for mass transfer to the solid phase. It was not possible to determine the effect of interfacial resistance in the solution process because of its complexity.

5. Closed-loop forced-convection systems are very satisfactory for mass transfer investigations of sparingly soluble materials. The idealized steady state condition can be closely approached and transient behavior studied if desired. Isothermal and nonisothermal conditions are easily established simultaneously in separate sections of a single system. The opportunity to study solution and deposition rates simultaneously is particularly important for investigating the transport mechanism. A wide continuous range of fluid velocities is easily obtained, and the velocity can be controlled extremely well.

6. Type-304 stainless steel is a suitable material for handling liquid lithium up to 1,100°F. because solution mass transfer rates are low. This condition minimizes the tendency for equipment failure by either corrosion or plugging.

ACKNOWLEDGMENT

The authors wish to thank the National Science Foundation for making this study possible.

Material supplied by M. S. A. Research Corporation, Crawford Fitting Company, and Olin Mathieson Chemical Corporation is gratefully acknowledged.

The assistance given by Volker Weiss concerning the metallurgical aspects of the study was very valuable.

NOTATION

A = area, sq. cm.
C = concentration of solute, g./cc.
C_P = heat capacity, cal./(g. °K.)
D_L = molecular diffusivity, sq.cm./sec.
j_d = $(k_L/V)[(\mu)/(\rho D_L)]^{2/3}$
k_c = reaction velocity constant, cm./sec.
k_L = liquid-phase mass tranfer coefficient, cm./sec.
k_s = solid-phase mass transfer coefficient, cm./sec.
K = distribution constant
L = plate length, cm.
N = local mass flux, g./(sq.cm.)(sec.)
N_T = total mass flux, g./sec.
q = heat flux, cal./(sq. cm.)(sec.)
r = radius, cm.
R = gas constant
T = temperature, °K.
t = time, sec.

Greek Letters

α = solution rate constant, cm./sec., over-all mass transfer coefficient
γ = activity coefficient
Δ = difference
θ = temperature difference, (To-Tw) °K.
κ = Boltzman constant (1.38×10^{-8} erg./°K.)
μ = viscosity, g./(cm.)(sec.)
ν = kinematic viscosity, sq.cm./sec.
ρ = density of liquid mixture, g./cc.

Dimensionless Groups

N_{Re} = Reynolds number for flat plate, $(V\rho L/\mu)$
N_{Sc} = Schmidt number $(\mu/\rho D_L)$

Subscripts

c = cross sectional
d = mass transfer
f = final value
K = K^{th} component
L = liquid phase
m = mean value
o = origin of coordinate system
p = peripheral
r = radial direction
s = solid phase
T = total
z = direction

Superscripts

o = equilibrium value
$*$ = interfacial value

LITERATURE CITED

1. Dana, A. W., O. H. Baker, and M. Ferguson, Technical Report III, ES 783, The Babcock and Wilcox Company (April 21, 1952).
2. Dana, A. W., *et al.*, Reports DC-52-27-45 (BW 5230) (May 1942) and DC-52-5-19 (August 20, 1952), The Babcock and Wilcox Company.
3. General Electric Co., Aircraft Nuclear Propulsion Project, Reports DC-51-9-36 (Sept. 1951) and DC-51-12-52 (Dec. 1951).
4. Hoffman, E. E., and W. D. Manly, "Corrosion Resistance of Metals and Alloys to Sodium and Lithium, Handling and Uses of the Alkali Metals," American Chemical Society (1957).
5. Epstein, L. F., *Proc. Intern. Congr. Peaceful Uses of Atomic Energy, Geneva, Aug. 1955*, **9**, 311 (1956).
6. Dunn, W. E., C. F. Bonilla, C. Ferstenberg, and B. Gross, *A.I.Ch.E. Journal*, **2**, 184 (1956).
7. Linton, W. H., and T. K. Sherwood, *Chem. Eng. Progr.*, **46**, 258 (1950).
8. Bennett, J. A. R., and J. B. Lewis, *A.I.Ch.E. Journal*, **4**, 418 (1958).
9. Higbie, Ralph, *Trans. Am. Inst. Chem. Engrs.*, **31**, 365 (1935).
10. Danckwerts, P. V., *Ind. Eng. Chem.*, **43**, 1460 (1951).
11. ———and Kennedy, *Trans. Inst. Chem. Engrs. (London)*, **32**, S49 (1954).
12. Bird, R. B., in "Advances in Chemical, Engineering," Vol. I, Academic Press, New York (1955).
13. Opfell, J. F., and B. H. Sage, *ibid.*
14. Jakob, Max, "Heat Transfer," Vol. I, John Wiley, New York (1949).
15. Sherwood, T. K., and R. L. Pigford, "Absorption and Extraction," McGraw-Hill, New York (1952).
16. Kàrmàn, Th. von, *Z. angew. Math. u. Mech.*, **1**, 233 (1921).
17. Bonilla, C. F., R. N. Roy-Choudhury, *et al.*, "Mass Transfer in Liquid Metal and Fused Salt Systems" NYO-3088, 3090, U.S.A.F.C. (1952).
18. Schlichting, Hermann, "The Boundary Layer Theory," Pergamon Press, New York (1955).
19. Bagley, K. Q., and K. R. Montgomery, United Kingdom Atomic Energy Authority, Report No. IGR-TN/C 250.
20. Sand, J., W. N. Gill, R. V. Jelinek, and C. S. Grove, "Solubility of Iron in Lithium," Syracuse University Research Institute Report (1958).

Manuscript received May 11, 1959; revision received June 26, 1959; paper accepted July 2, 1959. Paper presented at A.I.Ch.E. Kansas City meeting.